

# Time delay and duration of ionospheric total electron content responses to geomagnetic disturbances

J. Liu<sup>1,2</sup>, B. Zhao<sup>1</sup>, and L. Liu<sup>1</sup>

<sup>1</sup>Institute of Geology and Geophysics, Chinese Academy of Sciences, Beijing 100029, China

<sup>2</sup>Graduate University of Chinese Academy of Sciences, Beijing, China

Received: 15 September 2009 – Revised: 6 January 2010 – Accepted: 10 February 2010 – Published: 18 March 2010

**Abstract.** Although positive and negative signatures of ionospheric storms have been reported many times, global characteristics such as the time of occurrence, time delay and duration as well as their relations to the intensity of the ionospheric storms have not received enough attention. The 10 years of global ionosphere maps (GIMs) of total electron content (TEC) retrieved at Jet Propulsion Laboratory (JPL) were used to conduct a statistical study of the time delay of the ionospheric responses to geomagnetic disturbances. Our results show that the time delays between geomagnetic disturbances and TEC responses depend on season, magnetic local time and magnetic latitude. In the summer hemisphere at mid- and high latitudes, the negative storm effects can propagate to the low latitudes at post-midnight to the morning sector with a time delay of 4–7 h. As the earth rotates to the sunlight, negative phase retreats to higher latitudes and starts to extend to the lower latitude toward midnight sector. In the winter hemisphere during the daytime and after sunset at mid- and low latitudes, the negative phase appearance time is delayed from 1–10 h depending on the local time, latitude and storm intensity compared to the same area in the summer hemisphere. The quick response of positive phase can be observed at the auroral area in the night-side of the winter hemisphere. At the low latitudes during the dawn-noon sector, the ionospheric negative phase responses quickly with time delays of 5–7 h in both equinoctial and solstitial months.

Our results also manifest that there is a positive correlation between the intensity of geomagnetic disturbances and the time duration of both the positive phase and negative phase. The durations of both negative phase and positive phase have clear latitudinal, seasonal and magnetic local time (MLT) dependence. In the winter hemisphere, long durations for the positive phase are 8–11 h and 12–14 h during the daytime at middle and high latitudes for  $20 \leq A_p < 40$  and  $A_p \geq 40$ .

**Keywords.** Ionosphere (Equatorial ionosphere; Ionosphere-magnetosphere interactions; Ionospheric disturbances)

## 1 Introduction

Geomagnetic storms have profound influences on the ionosphere, leading to disturbances in the ionospheric F2 region. These disturbances involve enhancement and depletion in electron density, termed as positive and negative ionospheric storms, respectively. During geomagnetic storms the enhanced magnetospheric energy and energetic particles input into the polar upper atmosphere greatly modify the dynamic and chemical coupling processes of the thermosphere and ionosphere system, resulting in significant changes in electron density profile and total electron content (TEC) derived from global positioning system (GPS) network measurements. A number of excellent reviews have been published to summarize the current understanding of the ionospheric storms (e.g., Prölss, 1995; Buonsanto et al., 1999; Danilov and Laštovička, 2001; Mendillo, 2006).

Now it is generally believed that negative ionospheric storms are possibly caused by changes in the thermospheric composition due to the heating of the thermosphere during the geomagnetic storms. One of the significant features of the negative phase is its equatorward propagation during the storm from auroral latitudes towards lower latitudes. Several mechanisms have been considered as possible sources for the ionospheric positive phases (e.g., Danilov and Belik, 1992; Prölss, 1995), the F2-layer uplifting due to vertical drift, plasma fluxes from the plasmasphere and downwelling to the gas as a result of the storm-induced thermospheric circulation (Danilov and Laštovička, 2001). The altered thermospheric circulation causes downwelling of the neutral species through constant pressure surfaces at low–middle latitudes equatorward of the composition disturbance zone, increasing the O density relative to N<sub>2</sub> and O<sub>2</sub>. This produces increases in NmF2 and TEC (Fuller-Rowell et al., 1996).



Correspondence to: L. Liu  
(liul@mail.iggcas.ac.cn)

At low latitudes, another important factor that influences storm-time behavior of ionosphere are electric field disturbances including prompt penetration electric field (PPE) and wind disturbance dynamo electric field (DDE). Under effects of the PPE and DDE, the equatorial ionization anomaly (EIA) can undergo drastic modifications resulting in large ionospheric disturbances at low latitudes (e.g., Abdu et al., 1991). Occasionally, interplanetary electric field can continuously penetrate to the low latitudes ionosphere for many hours under storm conditions (e.g., Huang et al., 2005; Wei et al., 2008). Dramatic changes in the ionospheric vertical TEC are observed owing to the intense disturbances electric field associated with magneto-ionosphere interactions (Tsurutani et al., 2004). At low latitudes, the combined effects of wind field, the composition changes and electrodynamics make the ionospheric phenomena rather complex. Several mechanisms may work together to produce the observed phenomenon and their relative importance may differ from case to case and phase to phase of the storm. A study was designed to investigate the global signatures of ionospheric TEC making use of the GPS network for the first time during the geomagnetic storm (Ho et al., 1996, 1998). Astafyeva et al. (2007) developed a method for calculation of global or regional maps of velocities of TEC isolines displacements and investigation of TEC dynamics during the geomagnetically quiet and disturbance conditions. Numerous studies have investigated storm time ionospheric responses theoretically and observationally (e.g. Lee et al., 2004; Liu et al., 2002, 2004; Kutiev et al., 2005; Zhao et al., 2005, 2007; Maruyama and Nakamura, 2007; Astafyeva, 2009a, b).

It is generally believed that ionospheric storm has a close relationship with the thermospheric storm. The propagation of negative and positive ionospheric storms is strongly determined by the thermospheric disturbance spreading speed. More recently related papers have emerged, such as works finished by Sutton et al. (2009) where the total mass density measurements from the CHAMP satellite are used to evaluate the delayed thermospheric responses to the high latitude heating sources. A series of geomagnetic storms provide an opportunity to study the thermospheric responses to the high latitude heating, drawing the following conclusions: the time delay for the thermospheric density perturbations to the high latitude energy input is between 3–4 h at low latitudes while less than 2 h at middle latitudes to high latitudes, which are significantly shorter than those used in empirical models (Sutton et al., 2009).

A large amount of energy is deposited in high latitudes during the storms and substorms, which can generate traveling atmospheric disturbances (TADs) in the thermosphere (e.g., Richmond and Matsushita, 1975; Lu et al., 2001). The generated TADs propagate from high- to low- latitudes, even to the opposite hemisphere. The neutral winds perturbations associated with TADs can bring the plasma upward/downward along the magnetic field lines, resulting in ionospheric fluctuations, which are termed as

large scale traveling ionospheric disturbances (LSTIDs), attracting attention from observation and model studies (e.g., Afraimovich et al., 2002; Lee et al., 2004; Ding et al., 2007; Lei et al., 2008). LSTIDs, with horizontal velocities between 400 and 1000 m/s and periods in the range of 30 min to 3 h, are most likely the manifestations of atmospheric gravity waves launched by high latitude sources (Hunsucker, 1982). The LSTIDs generated during storms or substorms may show time delays at different stations along the propagation direction of TADs (e.g., Hunsucker, 1982; Hocke and Schlegel, 1996).

A study has been designed by Balan and Rao (1990) to investigate the dependence of the ionospheric response to the time of occurrence of sudden commencement (SC) and to the intensity of the magnetic storms for a low- and a middle latitude station by considering TEC for more than 60 SC-type geomagnetic storms. They found that the time delays of the positive phase are short for daytime SCs and long for nighttime SCs, whereas the opposite applies for the negative responses. The time delays are inversely related to the intensity of geomagnetic storms. Some estimates of time constants of the delayed reaction to the forcing geomagnetic activity for middle latitude F2 region are 0–6 h for positive disturbances, 12 h (Wrenn et al., 1987), 6–12 h (Forbes et al., 2000), 16–18 h (Kutiev and Muhtarov, 2001), and 8–20 h depending on seasons. The above time constants were obtained either from several ionosonde stations or from empirical models. However, global features such as the time of occurrence, time delay and duration as well as their relation to the intensity of the ionospheric storms have not received enough attention. This study will be the first attempt to investigate those global features of the ionospheric storms related to the geomagnetic disturbances by analyzing global TEC maps.

The rest of this paper is arranged as follows. In Sect. 2, we mainly discuss the data processing procedures and methods, followed by the results of the time delay of both positive and negative ionospheric storms with respect to the geomagnetic disturbances. The time durations will be addressed in Sect. 3. The analysis of the derived results is given and the conclusions are drawn in the last section.

## 2 Data selection and processing

The data we use are JPL-provided Ionosphere Maps exchange files (IONEX), which span from 28 August 1998 to 31 December 2008 (<http://cddis.gsfc.nasa.gov>). Before the day 307, 2002 each daily IONEX file contains 12 vertical TEC (VTEC) maps, starting from 01:00 UT to 23:00 UT. The newer daily files include 13 VTEC maps, starting from 00:00 UT to 24:00 UT, in order to facilitate the data interpolation. The VTEC is modeled in a solar-geomagnetic reference frame using bi-cubic splines on a spherical grid. It should be noted that although a Kalman filter is used to solve simultaneously for instrumental biases and VTEC on the grid (Pi

et al., 1997; Mannucci et al., 1998), the bias-removed line-of sight TEC obtained using the mapping technique has an uncertainty of about 1~2 TECU (Kil et al., 2003).

Every map is transformed into earth-fixed reference frame with a geographic longitude range from  $-180^\circ$  to  $180^\circ$  ( $5^\circ$  resolution) and geographic latitudes from  $-87.5^\circ$  to  $87.5^\circ$  ( $2.5^\circ$  resolution). Hourly value of TEC is obtained through a linear interpolation. The storm relative deviation of TEC (RTEC) is defined as follows:

$$\text{RTEC} = \frac{\text{TEC} - \text{TEC}_q}{\text{TEC}_q} \times 100\%$$

We choose a 27-day sliding smooth median value as  $\text{TEC}_q$ . The 24-hourly median values were obtained in each cell with a 27-day window and assigned to be the central 14th day. Then the window was moved forward one day and again the new hourly medians were assigned to next central day. Repeating this process, the median values were obtained for each cell on individual days from 28 August 1998 to 30 December 2008. On one hand, a 27-day running median is a natural choice as this period equals to one solar rotation; on the other hand, this saves us from large and unreal disturbance effects in the beginning and in the end of a month as well as at the junction of 2 months especially during the equinoctial periods when changes in the thermosphere and ionosphere are very fast (Mikhailov et al., 2004). The advantage of using running  $f_oF2$  median for F2-layer disturbance analyses was stressed long ago (e.g., Mednikova, 1957). A 27-day component is apparent in the solar EUV, due to the solar rotation, and in the many ionospheric parameters. Therefore, the 27-day sliding smooth median is used mainly to remove the solar cycle effects on the TEC. It has been also applied in many previous investigations.

We also interpolate the three hour  $A_p$  index into an hourly resolution. Because neither magnetospheric disturbances nor the positive and negative ionospheric storms exhibit well-defined onsets, we acquire the time delay between the  $A_p$  index, representing geomagnetic activity, and ionospheric response represented by RTEC through the cross-correlation function expressed as

$$C_{xy}(\tau) = \frac{\sum_i (x(t_i) - \bar{x})(y(t_i + \tau) - \bar{y})}{\sqrt{\sum_i (x(t_i) - \bar{x})^2 \sum_i (y(t_i + \tau) - \bar{y})^2}}$$

Here  $x$  and  $y$  represent the time series of two data sets, and  $\tau$  is the time delay between any two moments for which the respective values of  $x$  and  $y$  are cross-correlated.

The next step is to define a storm event and make a correlation analysis between the  $A_p$  index and RTEC. Taking into consideration  $A_p$  index presenting small short-duration peaks, we used a low-pass Butterworth filter with a window length of 12 h to smooth data sets and ensure that geomagnetic disturbances are long-lasting. As shown in Fig. 1a, there are a number of active geomagnetic events during the days 244–274 of the year 1998. The period between two

minima (circle) when filtered  $A_p \geq 20$  is considered. One of the criteria used in the selection of an event is based on the condition that the ionospheric response of individual storm is isolated (pre-storm conditions are beyond the scope of this paper). In some cases prior to the geomagnetic disturbances, the TEC is greatly enhanced for some hours, even up to a day (Burešová and Laštovička, 2007; Liu et al., 2008). Furthermore, we only consider the first one for consecutive storms reflected by filtered  $A_p$  index, as we suspect that the preconditioning environment may not reflect the state of the ionosphere caused by the current geomagnetic activity.

The lower panel of Fig. 1b gives examples of periods of magnetic disturbances and the associated negative and positive responses of TEC, as well as their cross-correlation function. The right panel shows a situation that causes the negative effect on TEC and the left panel of Fig. 1 applies for the opposite situation. We recorded the position of maximum and minimum values of the cross-correlation coefficient when  $\tau \geq 0$  and  $|C| \geq 0.4$ . The reason of choosing the above criterion is to ensure that the ionosphere is influenced by the recent geomagnetic disturbance and also guarantee the accuracy of the time delay. Then we make statistical results of position of this maximum and minimum in summer, winter and equinox. We employ the classification of Lloyd's seasons to define January, February, December and November as the winter months (Northern Hemisphere) and May, June, July and August as the summer months, and the rest as the equinox months.

In order to construct TEC maps, we follow the works of Codrescu et al. (2001) and Jee et al. (2004) to get TEC maps in the plane of magnetic local time (MLT) vs. magnetic latitudes (MLAT). Thus, we first transform the geographic longitude and latitude into MLT (00:00~24:00) and MLAT ( $-75^\circ \sim 75^\circ$ ), and divide the MLT vs. MLAT plane into mesh grids with a grid length  $d\text{MLAT}=1\text{h}$  and  $d\text{MLAT}=2.5^\circ$ . Then following the process described above, we can derive the mean time delays of positive and negative ionospheric storms effects.

### 3 Results of analysis

#### 3.1 Filtered $A_p$ distribution and storm intensity classification

Figure 2 shows the filtered  $A_p$  index distributions of the event numbers every month, storm intensity, and yearly and seasonal distribution. Figure 2a illustrates that the occurrence rate is higher in equinoctial months and lower around the solstice months which follow the semiannual variation of geomagnetic activity (e.g., Russell and McPherron, 1973). A majority of these events (710 out of 972) had maximum filtered  $A_p$  values between 20 and 40. The occurrence of yearly major geomagnetic disturbances is highest around the year 2000 which is around the time of maximum sunspot number.

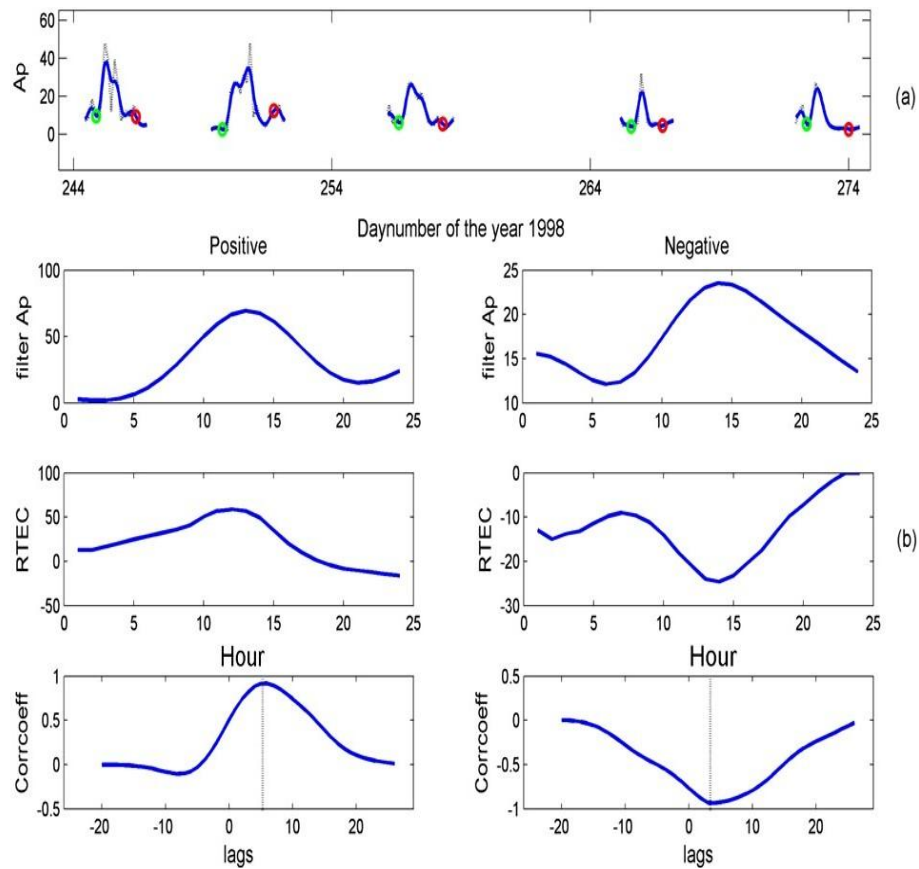


**Fig. 1.** (a) Geomagnetic activity during the 244th–274th days in the year 1998. (b) Example of a period of geomagnetic disturbance and associated positive and negative ionosphere responses RTEC, as well as their cross-related functions.

According to the filtered Ap, our statistical results were divided into two bins:  $20 \leq \text{Ap} < 40$  and  $\text{Ap} \geq 40$ , in order to get information regarding the intensity dependence of the ionospheric response. Figure 2d illustrates the classification of the filtered Ap index numbers in different seasons.

### 3.2 Negative storm time delay

Globally, we sum up all the time delay of negative ionospheric storms related to geomagnetic disturbances, as shown in Fig. 3. The upper panel of Fig. 3 illustrates the distributions of the mean time delay when the maximum filtered Ap index ranging from 20 to 40 in solstitial months (left two panels) and equinoctial months (right two panels) and the bottom two panel represents maximum filtered Ap index larger than 40. The Northern Hemisphere of the left two panels are associated with winter conditions. Here and in subsequent figures we combine the results for the winter and summer seasons by reversing geomagnetic latitude, omitting the difference in the same seasons as observed in different hemispheres and taking the average value of the time delay. This was done in order to have sufficient data for all local times globally.

As depicted in Fig. 3, the mean time delay of negative storm depends on season, latitude and local time, as well as the intensity of geomagnetic disturbance. In the summer hemisphere at mid- and high latitudes, it is evident that negative storm can propagate to the low latitudes at post-midnight to morning sector with time delay 4–7 h for both cases  $20 \leq \text{Ap} < 40$  and  $\text{Ap} \geq 40$ . As the earth rotates to the sunlight, negative phase retreats to higher latitudes and starts to extend to lower latitudes toward midnight sector. During the daytime and after sunset at mid- and low latitudes, the time delay is about 10 h for cases  $20 \leq \text{Ap} < 40$  and about 12 h for case  $\text{Ap} \geq 40$ . In the winter hemisphere, the situation is different in that the negative phase propagation time is delayed from 1–10 h depending on the local time, latitudes and storm intensity with respect to the same area in the summer hemisphere. For example, at post-midnight to morning sector at mid- and high latitudes, the delay time is 9–11 h, while at auroral latitudes during the night, the time delay for the negative phase is severely increased to around 13 h when  $20 \leq \text{Ap} < 40$  and 16 h when  $\text{Ap} \geq 40$ . During the daytime and after sunset at mid- and low latitudes, the delay time is 12 h for case  $20 \leq \text{Ap} < 40$  and 15–16 h for  $\text{Ap} \geq 40$ .

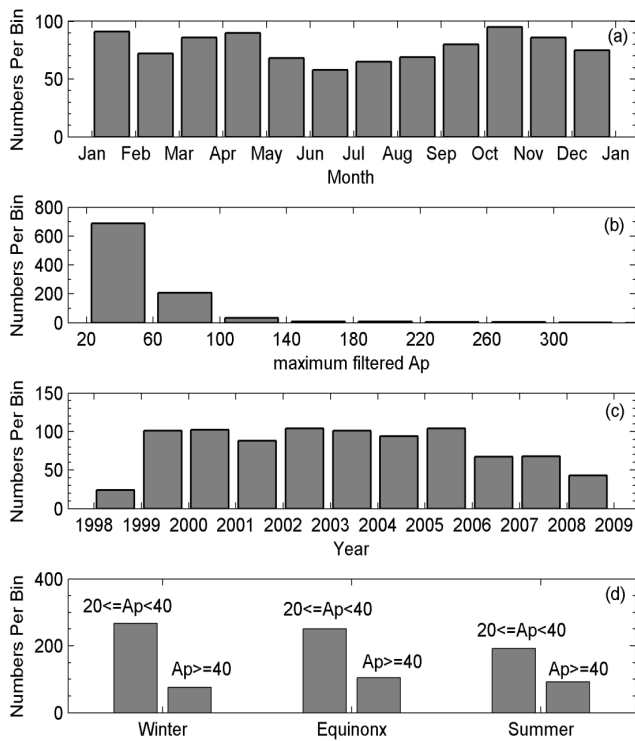


**Fig. 2.** (a) Total event numbers every month. (b) Distribution of the maximum filtered Ap. (c) Yearly event numbers of the geomagnetic disturbances. (d) Seasonal distribution of the filtered Ap in bins:  $20 \leq \text{filtered Ap} < 40$  and  $\text{filtered Ap} \geq 40$ .

The results of the mean time delay for the negative phase show an almost symmetric pattern about the magnetic equator in equinox. From dawn to noon sector, the negative phase propagates from high to middle latitudes with time delay 5–7 h. From morning to midnight sector at middle to low latitudes, the negative phase shows longer time delay, reaching values of 9–12 h and 13–15 h for situation  $20 \leq \text{Ap} < 40$  and  $\text{Ap} \geq 40$ , respectively. At the auroral latitudes in the night sector, the time delay for negative phase is postponed to around 12 h for situation  $20 \leq \text{Ap} < 40$  and around 16 h for  $\text{Ap} \geq 40$ .

A noteworthy phenomenon is presented at the low latitudes during the sunrise-noon sector. The ionospheric negative phase responses quickly with time delay of 5–7 h and longer in the afternoon sector both in equinoctial and solstitial months. There is no clear solar activity dependence of the mean time delay for negative ionospheric storms to geomagnetic disturbances.

### 3.3 Positive storm time delay

The mean time delays of positive ionospheric storm effects related to geomagnetic disturbances are plotted in Fig. 4. Generally, the ionosphere in daytime is more favorable for positive storm propagation with time delays of 4–5 h from high to middle latitudes in the winter and equinox which is

opposite to the situation for negative storm. Furthermore, there is no significant difference in the time delay with respect to the storm intensity. The areas where slow response, 10–14 h, of the positive storm effect appears are consistent with the quick response of the negative storm effect as shown in Fig. 3. In the winter hemisphere at middle latitudes, the quick response of the positive storm effect appears at 07:00–19:00 MLT while it appears in the summer hemisphere at 10:00–24:00 MLT for the case  $20 \leq \text{Ap} < 40$ . As the storm intensity increases for the case  $\text{Ap} \geq 40$ , the quick response of the positive storm effect appears at forenoon sector in the summer hemisphere and propagates to lower latitudes at both hemispheres. At auroral latitudes, the positive phase responds very quickly, especially in the winter and equinox at night sector with time delay 2–5 h. The time delay of positive storm in equinox shows almost the same pattern as in the winter hemisphere at the dayside.

Seasonal difference with respect to mean time delay of positive storm is not as evident as negative storms. Regarding to the latitude dependence, as latitude decreases, the time delay tends to increase from MLAT  $\sim 60^\circ$  to equatorial latitudes, reaching its maximum value for about 6–8 and 8–10 h for  $20 \leq \text{Ap} < 40$  and  $\text{Ap} \geq 40$ , respectively. The time lags of negative ionospheric storm responses to the geomagnetic disturbances show no evident dependence on the solar activity. The positive phases react to the geomagnetic storms faster at lower solar activity.

### 3.4 Time duration of negative phase and positive phase

Owing to the lack of a standard definition of an ionospheric storm, we arbitrarily define a storm event when the absolute RTEC exceed 15% consecutively for at least 3 h. Then we termed the length of the time series when the absolute RTEC exceed 15% as the time duration of the ionospheric storm. Figure 5 and 6 illustrate the features of the mean time durations for negative and positive storm phases, respectively, in the geomagnetic and magnetic local time frame. The time duration has clearly seasonal, latitudinal and storm intensity dependences. As shown in Fig. 5, in the summer the ionospheric negative phase can sustain for 9–10 and 15–16 h for the case  $20 \leq \text{Ap} < 40$  and  $\text{Ap} \geq 40$ , respectively, from high to middle latitudes, while in the winter the values are 9–10 and 10–12 h. In equinox, the durations are 9–10 and 9–15 h depending on the local time. As the latitude decreases mainly at mid-low and equatorial latitudes (from  $-30^\circ$  to  $30^\circ$ ), the ionospheric negative phase persists for shorter time about 5–8 h.

As depicted in Fig. 6, in the winter hemisphere, longest durations for the positive phase are 8–11 h and 12–14 h during the daytime at middle and high latitudes, and 11–12 and 15–16 h in the auroral area during the nighttime for the case  $20 \leq \text{Ap} < 40$  and  $\text{Ap} \geq 40$ . The duration time is relatively shorter, 6–8 and 7–9 h for the case  $20 \leq \text{Ap} < 40$  and  $\text{Ap} \geq 40$  at

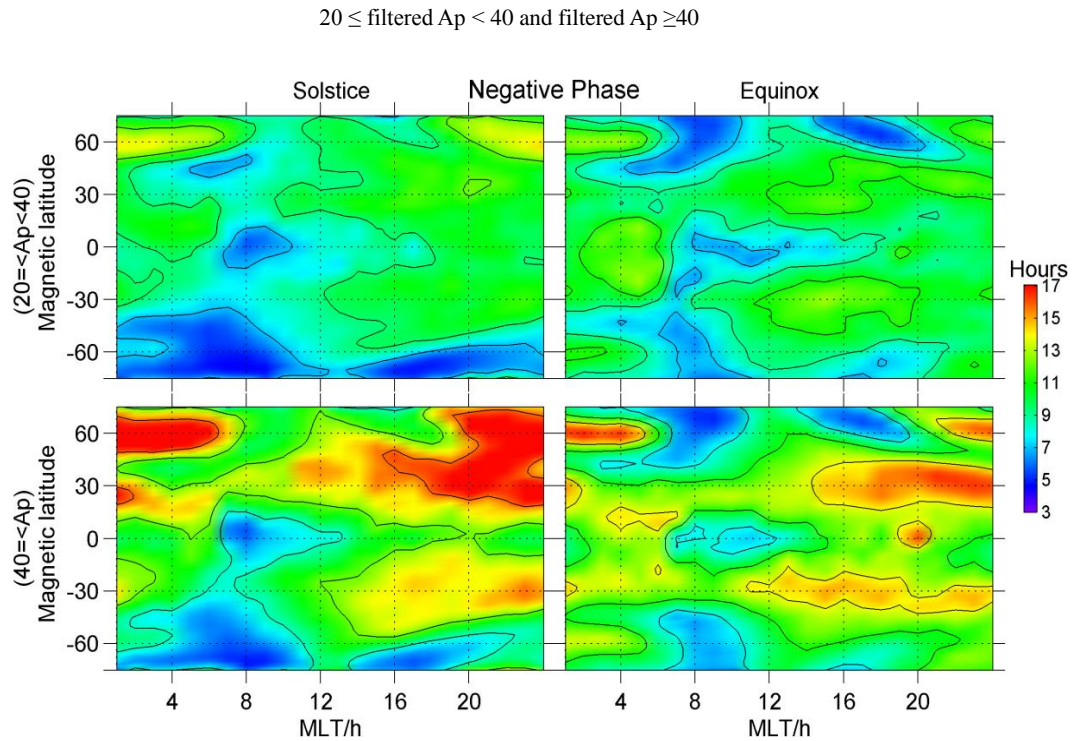


**Fig. 3.** Global distribution of the mean time delay related to negative ionospheric storms in the MLAT vs. MLT frame for solstitial months (left panels) and equinoctial months (right panels). The Northern Hemisphere of left panels locates in winter and the Southern Hemisphere corresponds to the summer months.

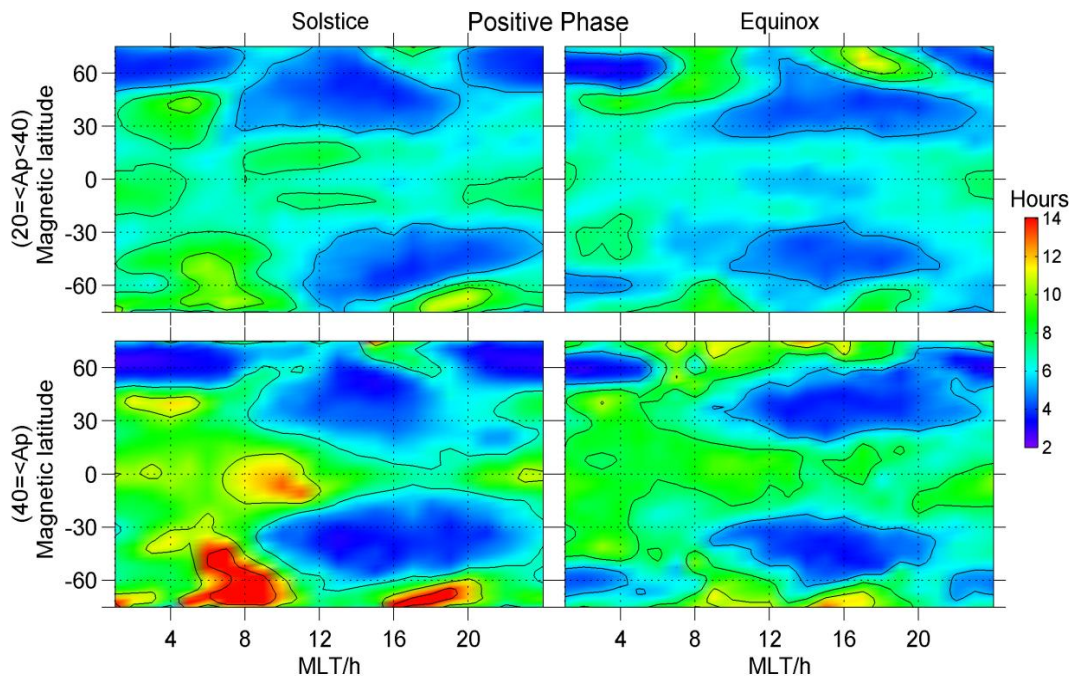


**Fig. 4.** Global distribution of the mean time delay related to positive ionospheric storms in the MLAT vs. MLT frame for solstitial months (left panels) and equinoctial months (right panels). The Northern Hemisphere of left panels locates in winter and the Southern Hemisphere corresponds to the summer months.

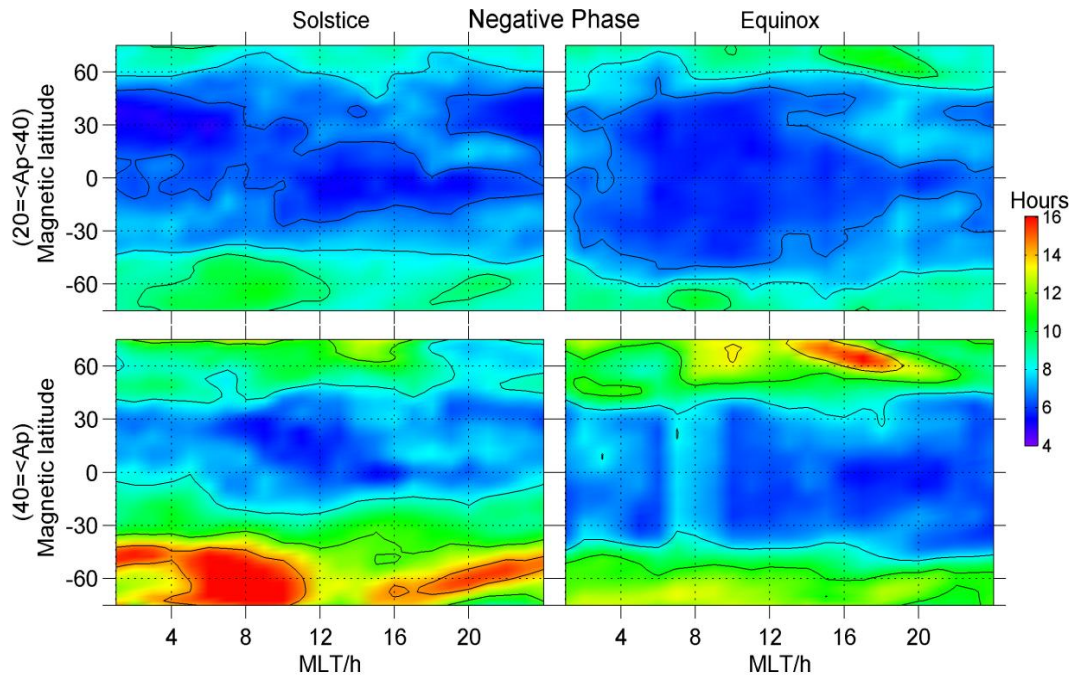


**Fig. 5.** Global distribution of the mean time duration related to negative ionospheric storms in the MLAT vs. MLT frame for solstitial months (left panels) and equinoctial months (right panels). The Northern Hemisphere of left panels locates in winter and the Southern Hemisphere corresponds to the summer months.

night at middle and low latitudes for both winter and summer hemispheres.

The time duration of the positive phase in equinox seems to have inconspicuous local time and latitudinal dependence compared with the observations during the solstitial months especially for the case  $20 \leq Ap < 40$ . Generally, the time duration is 7–8 h and 2–3 h longer at auroral and low areas during midnight to fore-morning sector, and also at mid-low latitudes in the post-sunset sector. An interesting feature to note is that at low latitudes in the daytime for equinoctial and solstitial months, the duration is also short-lived as depicted in Fig. 6.

The averaged time durations of the negative ionospheric storms tend to be longer at higher solar activity from middle to high latitudes ( $30^\circ$ – $75^\circ$ ) in solstitial months. However, the time durations of negative phases at low latitudes show less evident dependence on the solar activity. The positive ionospheric storms persist longer at higher solar activities.

#### 4 Discussion and conclusion

We have used of Ap index, representing the geomagnetic conditions, and JPL-provided TEC in order to evaluate the time delay and duration of ionospheric density variations during geomagnetically disturbed conditions. The main features are listed as follows: (1) In the summer hemisphere at mid- and high latitudes, negative storm can propagate to low

latitudes at post-midnight to morning sectors with time delays of 4–7 h. During sunlit hours, negative phase retreats to high latitudes and starts to extend to lower latitudes toward midnight sector with time delay 4–8 h as depicted in Fig. 3. (2) During daytime and after sunset at mid- and low latitudes, in the winter hemisphere, situation is different in that the negative phase appearance time is delayed from 1–10 h depending on the local time, latitudes and storm intensity with respect to the same area in the summer hemisphere. (3) A quick response of positive phase at the auroral area can be detected at the nightside of the winter hemisphere. (4) At the low latitudes in the sunrise-noon sector, the ionospheric negative phase responds quickly with time delay 5–7 h both in equinoctial and solstitial months. (5) As depicted in Fig. 6 in the winter hemisphere, long durations for the positive phase are 8–11 h and 12–14 h during the daytime in the middle and high latitudes. (6) In both equinoctial and solstitial months at low latitudes the positive phase persists for short time with time duration of 6–8 h. The positive storms show slightly longer time duration in the winter hemisphere than in the summer hemisphere.

As illustrated in Fig. 3 the negative phase can propagate more equatorward from midnight to morning sector, and then it gradually retreats to the high latitudes at the dayside, expanding towards low latitude again in the afternoon to middle night sector. Since the first suggestion by Seaton et al. (1956), it has been believed that the negative phase is caused by changes of the thermospheric composition due

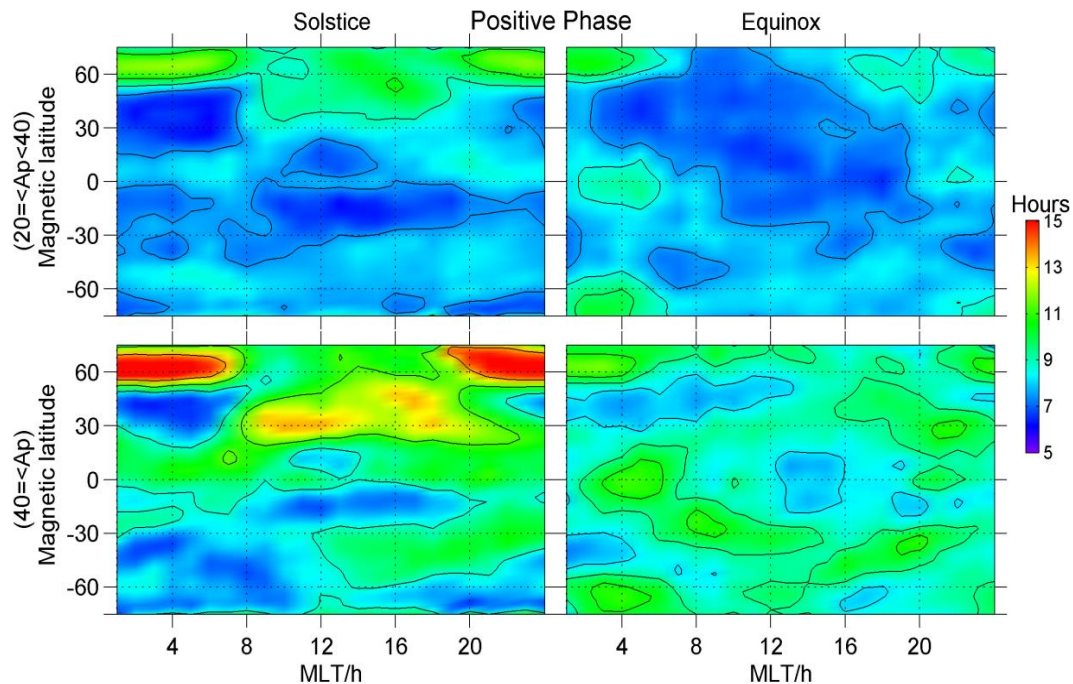


**Fig. 6.** Global distribution of the mean time duration related to positive ionospheric storms in the MLAT vs. MLT frame for solstitial months (left panels) and equinoctial months (right panels). The Northern Hemisphere of left panels locates in winter and the Southern Hemisphere corresponds to the summer months.

to heating of the thermosphere during geomagnetic disturbances (Danilov and Laštovička, 2001). In this way, abundant molecule gases in the lower thermosphere region are brought up which lead to a decrease in  $[O/N_2]$ , causing a depletion of TEC. According to Fuller-Rowell et al. (1994, 1996), this composition bulge is controlled by earth rotation, summer-to-winter circulation and diurnal variations of the wind field. During daytime the storm induced winds and the background day-to-night winds are out of phase, but in phase at night. Though nonlinear superposition, the composition bulge can be brought to lower latitudes faster in the night than in the daytime. So the time delay for negative phase is shorter in the nighttime than daytime in summer hemisphere as illustrated in Fig. 3.

During the daytime and after sunset at mid- and low latitudes, in the winter hemisphere, the negative phase appearance is delayed from 1–10 h depending on the local time, latitudes and storm intensity with respect to the same area in the summer hemisphere. Rodger et al. (1989) suggested that the seasonal effect is caused by the movement of the bulge by transequatorial summer-to-winter wind field. The summer-to-winter wind hinders the bulge propagation towards lower latitudes in winter and makes for the equatorward propagation in summer. That is why in the winter hemisphere, the negative phase propagation time in the same area is delayed with respect to that in the summer hemisphere.

There is no general agreement on what causes the long-duration positive phase. In our results the positive phase lasts for 9–10 h and 12–13 h during the daytime in the middle and high latitudes as illustrated in the left two panels of the winter hemisphere in Fig. 6. A Simulation based on thermosphere-ionosphere general circulation models suggest that this behaviour is due to composition changes (e.g. Burns et al., 1995; Fuller-Rowell et al., 1996). Increase in  $O/N_2$  ratio on a constant pressure surface has a strong correlation with long-term positive storm effects in electron density. However, other observations and simulation results demonstrate that meridional winds can also be the cause (e.g. Pröls, 1995; Bausker and Pröls, 1998). In these studies, the long-duration positive ionospheric storms are caused by upward transport of ionization, under the assumption of reduced loss rate of plasma at higher altitudes.

At low latitudes in the sunrise-noon sector, the ionospheric negative phase responds quickly with time delay of 5–7 h both in equinoctial and solstitial months. Low latitude ionospheric processes are significantly controlled by the electric field which, under quiet conditions, arises from the dynamo mechanism. During geomagnetic disturbed conditions, two broad types of disturbance electric fields could account for the observed major response features: (a) Direct penetration of magnetic and electric fields involving hydro-magnetic wave propagation similarly as in the storm sudden commencement phase or in substorm development and recovery

phase (Abdu et al., 1995). (b) Disturbance dynamo electric field produced by changes in the thermospheric circulation and neutral winds originating from storm energy deposition in the high latitude thermosphere (Rishbeth, 1975; Blanc and Richmond, 1980). During the daytime, the eastward electric field raises plasma to higher altitude from where plasma diffuses down along the magnetic line owing to the gravitational force and pressure gradient force. As a result, the equatorial dayside TEC will decrease and at the same time at off-equatorial latitudes will increase, forming the negative phase in the equatorial latitudes. Also background TEC values are rather low for the morning sector compared to the afternoon sector at the low latitudes which make the relative changes addressed in our study obvious. Both these factors contribute to the faster formation of negative ionospheric storm as depicted in the morning to noon sector in Fig. 3. Another possible reason is that TADs originate from both hemispheres, travelling with high velocity towards the low latitudes. As mentioned by Pröls (1993), 3–5 h after the sub-storm onset, a distinct increase in neutral density observed in low latitudes results from the combined compression and dissipation of the TADs energy. This energy increase is large enough to increase the temperature in upper atmosphere at low latitudes by 100 °K or more, leading to an increase in the loss rate of the plasma and corresponding reduction of TEC.

Because the dayside downward drifts caused by westward dynamo electric fields suppress the fountain effect and resulting in depletion of the anomaly crests (Scherliss and Fejer, 1997). Besides the electric fields, another way to modify equatorial anomaly is through wind-induced drifts. As mentioned by Burge et al. (1973), equatorward winds will oppose the poleward transportation of the ionization along the magnetic field lines. This will hinder the formation of the equatorial anomaly and generate negative storm effects in the anomaly crest regions. At the same time, the summer-to-winter winds bring ionization from upwind hemisphere to downwind hemisphere which can be used to explain the asymmetry in the time duration of the positive storm at low latitudes in solstice months.

At high latitudes or in auroral area, the fast positive storm effects during night, as illustrated in Fig. 2, may be caused by intense particle precipitation (Ho et al., 1998), especially in winter. Lower energy electrons are often observed to precipitate from the plasma sheet, from magnetosheath, and from magnetopause boundary layer (Labelle et al., 1978; Schumaker et al., 1989). A comprehensive survey (Newell et al., 1996) describes a number of satellite measurements of the flux of precipitating electrons as a function of magnetic local time. Electron precipitation associated with discrete auroral arcs occurs predominately in the 18:00–24:00 MLT sector. Previous observations show that during geomagnetic disturbance conditions, the particle precipitation will intensify and expand, causing positive storm effects at higher and lower latitudes (Essex and Watkins, 1973; Buonsanto et al., 1979).

It should be mentioned that the positive phase effect occurs earlier in the winter hemisphere than summer hemisphere. This asymmetry may be explained by the lower background values in the winter hemisphere than in the summer hemisphere that makes the relative change more evident.

The aim of this study is to give the average values of the time delay and duration in positive and negative TEC responses to geomagnetic activities. Our results can provide some useful supporting information when building empirical models. If accurate information on time delay and duration can be obtained, we can better understand the general variation pattern of the ionospheric TEC, which may aid weather forecasting. In addition, the fact is that the ionospheric TEC responses to geomagnetic activity have certain time delays during the geomagnetic storms, reminds us that ionospheric parameters are not only affected by the current but also by the past state of the geomagnetic activity. Thus when discussing the complex ionospheric phenomena, we should take into account both the current state and the past activity and consider also the interplay between them.

*Acknowledgements.* This research was supported by National Natural Science Foundation of China (40725014, 40804041) and National Important Basic Research Project (2006CB806306).

Topical Editor K. Kauristie thanks L. Sparks and another anonymous referee for their help in evaluating this paper.

## References

- Abdu, M. A., Sobral, J. H. A., Paula, E. R., and Batista, I. S.: Magnetospheric disturbance effects on the Equatorial Ionization Anomaly (EIA): an overview, *J. Atmos. Terr. Phys.*, 53, 757–771, 1991.
- Abdu, M. A., Batista, I. S., Walker, G. O., Sobral, J. H. A., Trivedi, N. B., and De paula, E. R.: Equatorial ionospheric electric fields during magnetospheric disturbances: local time/longitude dependences from recent EITS campaigns, *J. Atmos. Solar Terr. Phys.*, 57, 1065–1083, 1995.
- Afraimovich, E. L., Ashkaliev, Y. F., Aushev, V. M., Beletsky, A. B., et al.: Simultaneous radio and optical observations of the mid-latitude atmospheric response to a major geomagnetic storm of 6–8 April 2000, *J. Atmos. Sol. Terr. Phys.*, 64, 1943–1955, 2002.
- Astafyeva, E. I.: Dayside ionospheric uplift during strong geomagnetic storms as detected by the CHAMP, SAC-C, TOPEX and Jason-1 satellites, *Adv. Space Res.*, 43, 1749–1756, 2009a.
- Astafyeva, E. I.: Effects of strong IMF  $B_z$  southward events on the equatorial and mid-latitude ionosphere, *Ann. Geophys.*, 27, 1175–1187, 2009b, <http://www.ann-geophys.net/27/1175/2009/>.
- Astafyeva, E. I., Afraimovich, E. L., and Kosogorov, E. A.: Dynamics of total electron content distribution during strong geomagnetic storms, *Adv. Space Res.*, 39, 1313–1317, doi:10.1016/j.asr.2007.03.006, 2007.
- Balan, N. and Rao, P. B.: Dependence of the ionospheric response on the local time of sudden commencement and the intensity of the geomagnetic storms, *J. Atmos. Terr. Phys.*, 52, 269–275, 1990.

- Bauske, R. and Pröls, G. W.: Numerical simulation of long-duration positive ionospheric storm effects, *Adv. Space Res.*, 22, 117–121, 1998.
- Blanc, M. and Richmond, A. D.: The ionospheric disturbance dynamo, *J. Geophys. Res.*, 85, 1669–1686, 1980.
- Buonsanto, M. J., Mendillo, M., and Klobuchar, J. A.: The ionosphere at  $L=4$ : Average behavior and the response to geomagnetic storms, *Ann. Geophys.*, 35, 15–26, 1979.
- Burešová, D. and Laštovička, J.: Pre-storm enhancements of  $foF2$  above Europe, *Adv. Space Res.*, 39, 1298–1303, 2007.
- Burge, J. D., Eccles, D. J., King, W., and Rüster, R.: The effects of thermospheric winds on the ionosphere at low and middle latitudes during magnetic disturbances, *J. Atmos. Terr. Phys.*, 35, 617–623, 1973.
- Burns, A. G., Killeen, T. L., Deng, W., and Carignan, G. R.: Geomagnetic storm effects in the low- to middle-latitude upper thermosphere, *J. Geophys. Res.*, 100, 14673–14691, 1995.
- Codrescu, M. V., Beierle, K. L., Fuller-Rowell, T. J., Palo, S. E., and Zhang, X.: More total electron content climatology from TOPEX/Poseidon measurements, *Radio Sci.*, 36, 325–333, 2001.
- Danilov, A. D. and Belik, L. D.: Thermosphere composition and the positive phase of an ionospheric storm, *Adv. Space Res.*, 12, 257–260, 1992.
- Danilov, A. D. and Laštovička, J.: Effects of Geomagnetic storms on the ionosphere and atmosphere, *Int. J. Geomagn. Aero.*, 2, 209–224, 2001.
- Ding, F., Wan, W., Ning, B., and Wang, M.: Large-scale traveling ionospheric disturbances observed by GPS total electron content during the magnetic storm of 29–30 October 2003, *J. Geophys. Res.*, 112, A06309, doi:10.1029/2006JA012013, 2007.
- Essex, E. A., Mendillo, M., Schödel, J. P., et al.: A global response of the total electron content of the ionosphere to the magnetic storms of 17 December and 18 June 1972, *J. Atmos. Terr. Phys.*, 43, 293–306, 1981.
- Forbes, J. M., Palo, S. E., and Zhang, X.: Variability of the ionosphere, *J. Atmos. Solar Terr. Phys.*, 62, 685–693, 2000.
- Fuller-Rowell, T. J., Codrescu, M. V., Moffett, R. J., and Quegan, S.: Response of the thermosphere and ionosphere to the geomagnetic storms, *J. Geophys. Res.*, 99, 3893–3914, 1994.
- Fuller-Rowell, T. J., Codrescu, M. V., Rishbeth, H., Moffett, R. J., and Quegan, S.: On the seasonal response of the thermosphere and ionosphere to the geomagnetic storms, *J. Geophys. Res.*, 101, 2343–2353, 1996.
- Ho, C. M., Mannucci, A. J., Lindqwister, U. J., Pi, X., and Tsurutani, B. T.: Global ionosphere perturbations monitored by the Worldwide GPS Network, *Geophys. Res. Lett.*, 23(22), 3219–3222, 1996.
- Ho, C. M., Mannucci, A. J., Sparks, L., Pi, X., Lindqwister, U. J., Wilson, B. D., Iijima, B. A., and Reyes, M. J.: Ionospheric total electron content perturbations monitored by the GPS global network during two northern hemisphere winter storms, *J. Geophys. Res.*, 103, 26409–26420, 1998.
- Hocke, K. and Schlegel, K.: A review of atmospheric gravity waves and travelling ionospheric disturbances: 1982–1995, *Ann. Geophys.*, 14, 917–940, 1996, <http://www.ann-geophys.net/14/917/1996/>.
- Huang, C.-S., Foster, J. C., and Kelley, M. C.: Long-duration penetration of the interplanetary electric field to the low-latitude ionosphere during the main phase of magnetic storms, *J. Geophys. Res.*, 110, A11309, doi:10.1029/2005JA011202, 2005.
- Hunsucker, R. D.: Atmospheric gravity waves generated in the high latitude ionosphere: a review, *Rev. Geophys.*, 20, 293–315, 1982.
- Jee, G., Schunk, R. W., and Scherliss, L.: Analysis of TEC data from the TOPEX/ Poseidon mission, *J. Geophys. Res.*, 109, A01301, doi:10.1029/2003JA010058, 2004.
- Kil, H., Paxton, L. J., Pi, X., Hairston, M. R., and Zhang, Y.: Case study of the 15 July 2000 magnetic storm effects on the ionosphere-driver of the positive ionospheric storm in the winter hemisphere, *J. Geophys. Res.*, 108(A11), 1391, doi:10.1029/2002JA009782, 2003.
- Kutiev, I. and Muhtarov, P.: Modeling of midlatitude F region response to geomagnetic activity, *J. Geophys. Res.*, 106, 15501–15509, 2001.
- Kutiev, I., Watanabe, S., Otsuka, Y., and Saito, A.: Total electron content behavior over Japan during geomagnetic storms, *J. Geophys. Res.*, 110, A01308, doi:10.1029/2004JA010586, 2005.
- Labelle, J., Sica, R. J., Kletzing, C., Earle, G. D., Kelly, M. C., Lummerzheim, D. R., Torbert, B., Baker, K. D., and Berg, G.: Ionization from soft electron precipitation in the auroral F region, *J. Geophys. Res.*, 94, 3791–3798, 1989.
- Lee, C. C., Liu, J. Y., Chen, M. Q., Su, S. Y., Yeh, H. C., and Nozaki, K.: Observation and model comparisons of the traveling atmospheric disturbances over the Western Pacific region during the 6–7 April 2000 magnetic storm, *J. Geophys. Res.*, 109, A09309, doi:10.1029/2003JA010267, 2004.
- Lei, J., Burns, A. G., Tsugawa, T., Wang, W., Solomon, S. C., and Wiltberger, M.: Observations and simulations of quasiperiodic ionospheric oscillations and large-scale traveling ionospheric disturbances during the December 2006 geomagnetic storm, *J. Geophys. Res.*, 113, A06310, doi:10.1029/2008JA013090, 2008.
- Liu, L., Wan, W., Lee, C. C., Ning, B., and Liu, J. Y.: The low latitude ionospheric effects of the April 2000 magnetic storm near 120° E, *Earth Planets Space*, 56, 607–612, 2004.
- Liu, L., Wan, W., Ning, B., and Liu, J. Y.: Low latitude ionospheric effects near longitude 120° E during the great geomagnetic storm of July 2000, *Sci. In China*, 45, suppl., 148–155, 2002.
- Liu, L., Wan, W., Zhang, M., Zhao, B., and Ning, B.: Prestorm enhancements in  $NmF2$  and total electron content at low latitudes, *J. Geophys. Res.*, 113, A02311, doi:10.1029/2007JA012832, 2006.
- Lu, G., Richmond, D., Roble, R. G., and Emery, B. A.: Coexistence of ionospheric positive and negative storm phases under northern winter conditions: a case study, *J. Geophys. Res.*, 106, 24493–24504, doi:10.1029/2001JA000003, 2001.
- Mannucci, A. J., Tsurutani, B. T., Iijima, B. A., Komjathy, A., Saito, A., Gonzalez, W. D., Gurnieri, F. L., Konzyra, J. U., and Skoug, R.: Dayside global ionospheric response to the major interplanetary events of October 29–30, 2003 “Halloween Storms”, *Geophys. Res. Lett.*, 32, L12S02, doi:10.1029/2004GL021467, 2005.
- Maruyama, T. and Nakamura, M.: Conditions for intense ionospheric storms expanding to lower midlatitudes, *J. Geophys. Res.*, 112, A05310, doi:10.1029/2006JA012226, 2007.
- Mednikova, N. B.: Mid-latitude ionospheric disturbances, in *Physics of solar corpuscular fluxes and their impact on the upper atmosphere of the Earth*, p. 183, Acad. Press of USSR, Moscow, 1957 (in Russian).
- Mendillo, M.: Storms in the ionosphere: Patterns and processes for total electron content, *Rev. Geophys.*, 44, RG4001,

- doi:10.1029/2005RG000193, 2006.
- Mikhailov, A. V., Depueva, A. Kh., and Leschinskaya, T. Yu.: Observations of neutral winds and electric fields using backscatter from field-aligned irregularities, *Int. J. Geomagn. Aeron.*, 5, G11006, doi:10.1029/2003GI000058, 2004.
- Newell, P. T., Lyons, K. M., and Meng, C.-I.: A large survey of electron acceleration events, *J. Geophys. Res.*, 101, 2599–2614, 1996.
- Pi, X., Mannucci, A., Lindqwister, U. J., and Ho, C. M.: Monitoring of global ionospheric irregularities using the worldwide GPS network, *Geophys. Res. Lett.*, 24, 2283–2286, 1997.
- Prölss, G. W.: Ionospheric F-region storms, in *handbook of Atmospheric electrodynamics*, 2, 195, CRC press, Boca Ration, Fla, 1995.
- Prölss, G. W.: Common origin of positive ionospheric storms at middle latitudes and geomagnetic activity effects at low latitudes, *J. Geophys. Res.*, 98, 5981–5991, 1993.
- Richmond, A. D. and Matsushita, S.: Thermospheric response to a magnetic substorm, *J. Geophys. Res.*, 80, 2839–2850, 1975.
- Rishbeth, H.: F-region storms and thermospheric circulation, *J. Atmos. Terr. Phys.*, 37, 1055–1064, 1975.
- Rodger, A. S., Wrenn, G. L., and Rishbeth, H.: Geomagnetic storms in the Antarctic F-region, II, Physical interpretation, *J. Atmos. Terr. Phys.*, 51, 851–866, 1989.
- Russell, C. T. and McPherron, R. L.: Semiannual variation of geomagnetic activities, *J. Geophys. Res.*, 78, 92–108, 1973.
- Scherliess, L. and Fejer, B. G.: Storm time dependence of equatorial disturbance dynamo zonal electric fields, *J. Geophys. Res.*, 102, 24037–24046, 1997.
- Schumaker, T. L., Gussenhoven, M. S., Hardy, D. A., and Carovillano, R. L.: The relationship between diffuse auroral and plasmasheet electron distributions near localmidnight, *J. Geophys. Res.*, 94, 10061–10078, 1989.
- Seaton, M. J.: A possible explanation of the drop in F-region critical densities accompanying major ionospheric storms, *J. Atmos. Terr. Phys.*, 8, 122–124, 1956.
- Sutton, E. K., Forbes, J. M., and Knipp, D. J.: Rapid response of the thermosphere to variations in Joule heating, *J. Geophys. Res.*, 114, A04319, doi:10.1029/2008JA013667, 2009.
- Tsurutani, B. T., Mannucci, A., Iijima, B., Abdu, M. A., et al.: Global dayside ionospheric uplift and enhancement associated with interplanetary electric fields, *J. Geophys. Res.*, 109, A08302, doi:10.1029/2003JA010342, 2004.
- Wei, Y., Hong, M., Wan, W., Du, A., Lei, J., Zhao, B., Wang, W., Ren, Z., and Yue, X.: Unusually long lasting multiple penetration of interplanetary electric field to equatorial ionosphere under oscillating IMF Bz, *Geophys. Res. Lett.*, 35, L02102, doi:10.1029/2007GL032305, 2008.
- Wrenn, G. L., Rodger, A. S., and Rishbeth, H.: Geomagnetic storms in the Antarctic F region. I. Diurnal and seasonal patterns for main phase effects, *J. Atmos. Terr. Phys.*, 49, 901–913, 1987.
- Zhao, B., Wan, W., and Liu, L.: Responses of equatorial anomaly to the October–November 2003 superstorms, *Ann. Geophys.*, 23, 693–706, 2005, <http://www.ann-geophys.net/23/693/2005/>.
- Zhao, B., Wan, W., Liu, L., and Mao, T.: Morphology in the total electron content under geomagnetic disturbed conditions: results from global ionosphere maps, *Ann. Geophys.*, 25, 1555–1568, 2007, <http://www.ann-geophys.net/25/1555/2007/>.